

Direct and converse flexoelectricity in two-dimensional materials

Matteo Springolo,¹ Miquel Royo,¹ and Massimiliano Stengel^{1,2}

¹*Institut de Ciència de Materials de Barcelona (ICMAB-CSIC), Campus UAB, 08193 Bellaterra, Spain*

²*ICREA - Institució Catalana de Recerca i Estudis Avançats, 08010 Barcelona, Spain*

(Dated: October 18, 2021)

Building on recent developments in electronic-structure methods, we define and calculate the flexoelectric response of two-dimensional (2D) materials fully from first principles. In particular, we show that the open-circuit voltage response to a flexural deformation is a fundamental linear-response property of the crystal that can be calculated within the primitive unit cell of the flat configuration. Applications to graphene, silicene, phosphorene, BN and transition-metal dichalcogenide monolayers reveal that two distinct contributions exist, respectively of purely electronic and lattice-mediated nature. Within the former, we identify a key *metric* term, consisting in the quadrupolar moment of the unperturbed charge density. We propose a simple continuum model to connect our findings with the available experimental measurements of the converse flexoelectric effect.

Among their many prospective applications, two-dimensional (2D) materials have received, in the last few years, considerable attention as a basis for novel electromechanical device concepts, such as sensors or energy harvesters. [1, 2] Such an interest has stimulated intense research, both experimental and theoretical, to characterize the fundamentals of electromechanical couplings in monolayer (or few-layer) graphene, [3, 4] boron nitride [5, 6] and transition-metal dichalcogenides. [1, 7] For the most part, efforts were directed at understanding piezoelectric and piezotronic properties [1] with stretchable/tunable electronics in mind; more recently flexoelectricity has been attracting increasing attention. [2, 8]

Flexoelectricity, describing the coupling between a strain gradient and the macroscopic polarization, [9, 10] is expected to play a prominent role in 2D crystals due to their extreme flexibility. Recently, several experimental works [4, 7, 8] reported a significant out-of-plane electromechanical response in graphene, BN, transition-metal dichalcogenides (TMDs) and related materials. Experiments were generally performed via piezoelectric force microscopy (PFM), which probes the *converse* effect (deformations in response to an applied voltage) in terms of an effective piezoelectric coefficient, d_{33}^{eff} . How the measured values of d_{33}^{eff} relate to the intrinsic flexoelectric coefficients of the 2D layer is, however, currently unknown. First, experiments are usually performed on supported layers; [7, 8] this implies a suppression of their mechanical response due to substrate interaction, [11] whose impact on d_{33}^{eff} remains poorly understood. Second, flexoelectricity is a non-local effect, where electromechanical stresses depend on the *gradients* of the applied external field; this substantially complicates the analysis compared to the piezoelectric case, where spatial inhomogeneities in the tip potential play little role. [12] In fact, even understanding what components of the 2D flexoelectric tensor contribute to d_{33}^{eff} is far from trivial. [7] Unless these questions are settled by establishing reliable models of the converse flexoelectric effect in 2D crystals,

the analysis of the experimental data remains to a large extent speculative, which severely limits further progress towards a quantitative understanding.

Theoretical simulations are a natural choice to shed some light on the aforementioned issues. Several groups have studied flexoelectricity in a variety of monolayer crystals including graphene, hexagonal BN, and transition metal dichalcogenides; calculations were performed either from first principles [3, 5, 13–16] or by means of classical force fields. [17, 18] Most authors, however, have defined and calculated the flexoelectric coefficient as a dipolar moment of the deformed layer, which has two main shortcomings. First, calculating the dipole moment of a curved crystalline slab is not free from ambiguities [19], and this has resulted in a remarkable scattering of the reported results. Second, such a definition has limited practical value, unless its relationship with the experimentally relevant parameters (electric fields and potentials) is established. The latter issue may appear insignificant at first sight, but should not be underestimated, as the Poisson equation of electrostatics is modified by curvature in a nontrivial way. [20] Some controversies around the thermodynamic equivalence between the direct and converse flexoelectric effect [21, 22] complicate the situation even further, calling for a fundamental solution to the problem. Thanks to the progress of the past few years in the computational methods, [20, 23–28] addressing these questions in the framework of first-principles linear-response theory appears now well within reach.

Here we overcome the aforementioned limitations by defining and calculating flexoelectricity as the open-circuit voltage response to a flexural deformation (“flexovoltage”) of the 2D crystal in the linear regime. Building on the recently-developed implementation of bulk flexoelectricity in 3D, [28, 29] we show that the flexovoltage coefficient, φ , is a fundamental linear-response property of the crystal, and can be calculated by using the primitive 2D cell of the unperturbed flat layer.

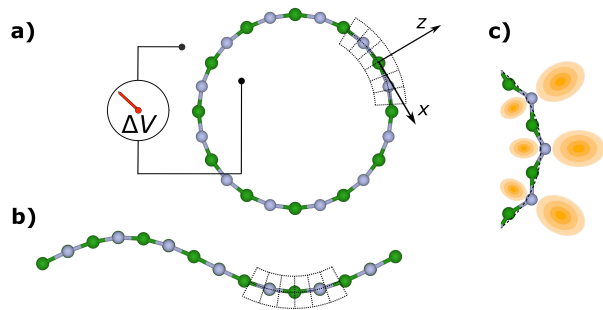


FIG. 1. Schematic illustration of the flexoelectric response in BN. (a): Cross-section of a BN nanotube; the voltage drop between its inner and outer sides is highlighted. (b): Flexural phonon, corresponding to an in-plane modulation of the same strain field as in (a). (c): Lattice-mediated and purely electronic effects contributing to the dipole. Gray/green circles represent the B/N atoms. The deformed electronic orbitals are shown as yellow shaded ellipses.

We demonstrate our method by studying several monolayer materials as testcases (C, Si, P, BN, MoS₂, WSe₂ and SnS₂), which we validate against direct calculation of nanotube structures. We find that the overall response consists in two well-defined contributions, a clamped-ion (CI) and a lattice-mediated (LM) term, in close analogy with the theory of the piezoelectric response. [30] At the CI level, our calculations show a remarkable cancellation between a dipolar linear-response term and a previously overlooked “metric” contribution, which we rationalize in terms of an intuitive toy model of noninteracting neutral spheres. [20, 25] We further demonstrate that φ describes both the direct and converse coupling between local curvature and transverse electric fields in an arbitrary geometry, ranging from nanotubes to flexural phonons and rippled layers. Based on this result, we build a quantitatively predictive model of a flexoelectric layer on a substrate, and we use it to discuss recent experimental findings.

The fundamental quantity that we shall address here is the voltage drop across a thin layer due to a flexural deformation, where the latter is measured by the radius of curvature, R . At the leading order, the voltage drop is inversely proportional to R ,

$$\Delta V = \frac{\varphi}{R} + O(R^{-2}), \quad \varphi = \frac{\mu^{2D}}{\epsilon_0}, \quad (1)$$

where φ can also be expressed as a 2D flexoelectric coefficient (in units of charge, describing the *effective* dipole per unit area that is linearly induced by a flexural deformation) divided by the vacuum permittivity, ϵ_0 . Our goal is to calculate the constant of proportionality, φ , which we shall refer to as “flexovoltage” coefficient.

The underlying physical model is that of a nanotube of radius R constructed by bending a flat layer, as illustrated in Fig.1(a); the voltage drop between the interior

and the exterior is then given by Eq. (1). Another obvious example is that of a long-wavelength flexural phonon [see Fig. 1(b)]. Due to rotational invariance, the modulated strain field locally recovers the same pattern as in Fig.1(a). [See Ref. 20 and Sec. 2.8.2 of Ref. 25.] At the leading order in the wave vector, \mathbf{q} this results in a local jump in the electrostatic potential across the layer of

$$\Delta V(x, y) = \varphi K(x, y), \quad (2)$$

where the local inverse radius of curvature, $K(x, y) = -\nabla^2 u_z(x, y)$, is given by the Laplacian of the vertical displacement field, u_z . [31] As we shall see shortly, the effect originates from the distortion of both the electronic cloud and the crystal structure [Fig.1(c)].

To express the flexovoltage as a linear-response property, we start by associating the flexural deformation with a mapping between the Cartesian frame of the flat layer, and the curvilinear frame of the bent nanotube [dashed grid in Fig.1(a)]. In a neighborhood of the nanotube surface, such a mapping corresponds to a strain field with cylindrical symmetry, of the type $\varepsilon_{xx}(z) = z/R$, where \hat{z} is the normal to the layer surface, \hat{x} runs over the tangential direction, and $\varepsilon_{\alpha\beta}$ is the symmetric strain tensor. This results in a macroscopic transverse strain gradient $\varepsilon_{xx,z} = \partial\varepsilon_{xx}/\partial z = 1/R$, whose amplitude is the inverse radius of curvature, [25, 32] and will play the role of the perturbative parameter, λ , henceforth.

To discuss the electrostatic potential, which defines the open-circuit voltage φ , we shall frame our arguments on the Poisson equation in the curvilinear frame of the bent layer, following the guidelines of Refs. 20, 25, and 32,

$$\nabla \cdot (\boldsymbol{\epsilon} \cdot \mathbf{E}) = \rho, \quad \boldsymbol{\epsilon} = \epsilon_0 \sqrt{g} \mathbf{g}^{-1}. \quad (3)$$

The main difference with respect to the Cartesian formulation is that the vacuum permittivity here becomes a tensor that depends on the metric of the deformation, \mathbf{g} . Within the linear regime, one can write $\rho = \rho^{(0)} + \lambda\rho^{(1)} + \dots$, where $\rho^{(0)}$ is the unperturbed density and $\rho^{(1)}$ the first-order response in λ . (For the time being we shall assume that $\rho^{(1)}$ refers to the static response, inclusive of electronic and ionic relaxations.) We find that the open-circuit potential φ is given by

$$\varphi = \frac{\mathcal{D}[\rho^{(1)}]}{\epsilon_0} + \varphi^M, \quad \varphi^M = -\frac{\mathcal{Q}[\rho^{(0)}]}{2\epsilon_0}, \quad (4)$$

where

$$\mathcal{D}[f] = \int dz z f(z) \quad \mathcal{Q}[f] = \int dz z^2 f(z). \quad (5)$$

indicate the first (dipolar) and second (quadrupolar) moment of the function f along the out-of-plane direction z , and $\rho^{(0)}(z)$ and $\rho^{(1)}(z)$ are the in-plane averages of the respective microscopic response functions. $\mathcal{D}[\rho^{(1)}]$ corresponds to the λ -derivative of the “radial polarization”

(\mathbf{p}) as defined in Ref. 19; the second term in Eq. (4) is a *metric* contribution that only depends on the unperturbed density $\rho^{(0)}$, and originates from the linear variation of ϵ in Eq. (3). As we shall see shortly, the dipolar linear-response part is always large and negative, while the metric term is large and positive, typically leading to an almost complete mutual cancellation.

The challenging part of the problem consists in computing the dipolar linear-response contribution. To facilitate our progress towards a practical method, we shall use $\rho^{(1)} = -\nabla \cdot \mathbf{P}^{(1)}$, where $\mathbf{P}^{(1)}$ is the microscopic *polarization* response to the deformation. (The zero-th moment of $P_z^{(1)}$ along z yields $\mathcal{D}[\rho^{(1)}]$, after an integration by parts.) Then, by using the formulation of Ref. [20], we can write the radial component of $\mathbf{P}^{(1)}$ as

$$P_z^{(1)}(z) = zP_{z,xx}^U(z) + P_{zz,xx}^G(z). \quad (6)$$

The cell-periodic response functions $P_{z,xx}^U(z)$ and $P_{zz,xx}^G(z)$ (in-plane averaging is assumed) have the physical interpretation of a *local* piezoelectric (U) and flexoelectric (G) coefficient. [32] The rationale behind such a decomposition is rooted on the availability of efficient first-principles methods to calculate both terms in Eq. (6), as we shall illustrate in the following.

To perform the actual calculations, we shall accommodate the unperturbed (flat) monolayer in a standard supercell, where the out-of-plane dimension L is treated as a convergence parameter. Regarding the gradient (G) contribution, we find

$$\varphi^G = \frac{1}{\epsilon_0} \int dz P_{zz,xx}^G(z) = \frac{L}{\epsilon_0 \epsilon_{zz}} \mu_{zz,xx}, \quad (7)$$

where ϵ_{zz} is the out-of-plane component of the macroscopic dielectric tensor, and $\mu_{zz,xx}$ is the transverse component of the flexoelectric tensor of the supercell. Clearly, both $\mu_{zz,xx}$ and ϵ_{zz} depend on L (averaging over an arbitrary supercell volume is implied, and short-circuit electrical boundary conditions are usually imposed [28] in the calculation of μ). However, they do so in such a way that their ratio multiplied by L does not (assuming that L is large enough to consider the repeated layers as nonoverlapping). Regarding the contribution of the first term on the rhs of Eq. (6), we have

$$\varphi^U = \frac{\mathcal{D}[P_{z,xx}^U]}{\epsilon_0} = \frac{\mathcal{Q}[\rho_{xx}^U]}{2\epsilon_0}, \quad (8)$$

where $\rho_{xx}^U(z)$ is the first-order charge-density response to a uniform strain ($\rho_{xx}^U = -\partial P_{z,xx}^U / \partial z$). The total flexovoltage of the slab is then given by

$$\varphi = \frac{dV}{d\lambda} = \varphi^G + \varphi^U + \varphi^M, \quad (9)$$

where neither of φ^G , φ^U or φ^M depend on L , and should therefore be regarded as well-defined physical properties

of the isolated monolayer. One can verify that, by applying the present formulation to crystalline slabs of increasing thickness, we recover the results of Ref. 32 once φ is divided by the slab thickness, t , and the thermodynamic limit performed. (φ^G and $\varphi^U + \varphi^M$ tend to the bulk and surface contributions to the total flexoelectric effect, respectively.)

Eq. (9) is directly suitable for a numerical implementation, as it only requires response functions that are routinely calculated within density-functional perturbation theory (DFPT). The partition between ‘‘G’’ and ‘‘U’’ contributions, however, is hardly meaningful for an atomically thin 2D monolayer, where essentially everything is surface and there is no bulk underneath. Thus, we shall recast Eq. (9) in a more useful form hereafter, by seeking a separation between clamped-ion (CI) and lattice-mediated (LM) effects instead [Fig. 1(b)],

$$\varphi = \varphi^{\text{CI}} + \varphi^{\text{LM}}. \quad (10)$$

We find [31] that the CI contribution has the same functional form as the total response,

$$\varphi^{\text{CI}} = \frac{L}{\epsilon_0 \bar{\epsilon}_{zz}} \bar{\mu}_{zz,xx} + \frac{\mathcal{Q}[\bar{\rho}_{xx}^U]}{2\epsilon_0} - \frac{\mathcal{Q}[\rho^{(0)}]}{2\epsilon_0}, \quad (11)$$

with the only difference that the flexoelectric (μ), dielectric (ϵ_{zz}) and uniform-strain charge response (ρ^U) functions have been replaced here with their clamped-ion counterparts, indicated by barred symbols. Regarding the LM part,

$$\varphi^{\text{LM}} = \frac{1}{S\epsilon_0} \hat{Z}_{\kappa\alpha}^{(z)} \hat{\Phi}_{\kappa\alpha,\kappa'\beta}^{-1} \hat{C}_{\beta z,xx}^{\kappa'}, \quad (12)$$

we have a more intuitive description in terms of the out-of-plane *longitudinal* charges $\hat{Z}_{\kappa\alpha}^{(z)} = Z_{\kappa\alpha}^{(z)} / \bar{\epsilon}_{zz}$, the pseudoinverse [33] of the zone-center dynamical matrix, $\hat{\Phi}_{\kappa\alpha,\kappa'\beta}^{-1}$, and the atomic force response [31] to a flexural deformation of the slab, $\hat{C}_{\beta z,xx}^{\kappa}$. Note that the ‘‘mixed’’ contribution [24] to the bulk flexoelectric tensor exactly cancels [31] with an equal and opposite term in the lattice-mediated contribution to φ^U , hence its absence from Eq. (10).

Our calculations are performed in the framework of density-functional perturbation theory [34, 35] (DFPT) within the local-density approximation, as implemented in ABINIT [29, 36]. (Computational parameters and extensive tests, including calculations performed within the generalized-gradient approximation, are described in Ref. 31). In Table I we report the calculated bending flexovoltages for several monolayer crystals. Both the CI and LM contributions show a considerable variety in magnitude and sign: while the former dominates in the TMDs, the reverse is true for BN, and SnS₂ seems to lie right in the middle. The case of phosphorene is interesting: its lower symmetry allows for a nonzero φ^{LM} in spite of it being an elemental crystal like C and Si; it also

| | φ^{CI} | φ^{LM} | φ |
|------------------|-----------------------|-----------------------|-----------|
| C | -0.1134 | 0.0000 | -0.1134 |
| Si | 0.0585 | 0.0000 | 0.0585 |
| P (zigzag) | 0.2320 | -0.0151 | 0.2170 |
| P (armchair) | -0.0130 | -0.0461 | -0.0591 |
| BN | -0.0381 | -0.1628 | -0.2009 |
| MoS ₂ | -0.2704 | -0.0565 | -0.3269 |
| WSe ₂ | -0.3158 | -0.0742 | -0.3899 |
| SnS ₂ | 0.1864 | 0.1728 | 0.3592 |

TABLE I. Clamped-ion (CI), lattice-mediated (LM) and total flexovoltages (nV·m) of the 2D crystals studied in this work. Due to its lower symmetry, for phosphorene two independent bending directions (armchair and zigzag) exist.

allows for a substantial anisotropy of the response. If we assume a physical thickness t corresponding to the bulk interlayer spacing, we obtain an estimate (see Table 6 of Ref. 31) for the volume-averaged flexoelectric coefficients, of $|\mu| = |\mu^{2\text{D}}|/t \sim 1 - 5$ pC/m. (μ , unlike $\mu^{2\text{D}}$, is inappropriate [19] for 2D layers given the ill-defined nature of the parameter t ; we use it here for comparison purposes only.) This value is in the same ballpark as earlier predictions, [13, 15–17] although there is a considerable scatter in the latter. For example, the value quoted by Ref. [17] for graphene is very close to ours, but their results for other materials are either much larger (TMD’s, silicene) or much smaller (BN); other works tend to disagree both with our results and among themselves. These large discrepancies are likely due to the specific computational methods that were adopted in each case (often the total dipole moment of a bent nanoribbon including the boundaries was calculated, rather than the intrinsic response of the extended layer), or to the aforementioned difficulties [19] with the definition of the dipole of a curved surface.

Very recently Ref. [19] reported first-principles calculations of some of the materials presented here by using methods that bear some similarities to ours, which allows for a more meaningful comparison. By converting our results for Si and C to the units of Ref. [19] via Eq. (1), we obtain $\mu_{\text{C}} = -0.0063e$ and $\mu_{\text{Si}} = +0.0032e$; these, however, are almost two orders of magnitude smaller, and with inconsistent signs, with respect to the corresponding results of Ref. [19]. We ascribe the source of disagreement to the neglect in Ref. [19] of the metric term in Eq. (11). Indeed, for the dipolar linear-response contribution [first two terms in Eq. (11)] we obtain $\mu_{\text{C}}^{\text{dip}} = -0.22e$ and $\mu_{\text{Si}}^{\text{dip}} = -0.19e$, now in excellent agreement (except for the sign) with the results of Codony *et al.*. This observation points to a nearly complete cancellation between the dipolar and metric contribution to φ , which is systematic

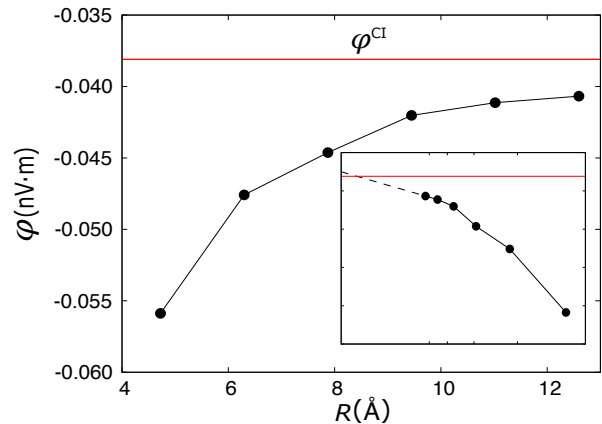


FIG. 2. Clamped-ion flexovoltage coefficient calculated as $\varphi = \Delta V R$, plotted as a function of the nanotube radius R . Our linear-response result [Eq. (11)] is shown as a red line. The inset shows φ as a function of $1/R$, the dashed line being a linear extrapolation from the last two calculated points to $R \rightarrow \infty$.

across the whole materials set (see Table 3 of Ref. [31]).

To clarify this point, we have performed additional calculations on toy model, consisting of a hexagonal layer of well-spaced rare gas atoms. [31] This is a system where no response should occur, as an arbitrary “mechanical deformation” consists in the trivial displacement of non-interacting (and spherically symmetric) neutral atoms. We find that φ^{dip} and φ^{met} are, like in other cases, large and opposite in sign; this, however, is just a side-effect of the coordinate transformation (i.e., a mathematical artefact), and does not reflect a true physical response of the system to the perturbation. For a lattice parameter that is large enough, the cancellation becomes exact and our calculated value of φ vanishes as expected on physical grounds. This further corroborates the soundness of our definition of $\mu^{2\text{D}}$, which is based on the electrostatic potential. The latter, in addition to being an experimentally relevant parameter, behaves as a true scalar under a coordinate transformation; it is therefore unaffected, unlike the charge density, by the (arbitrary) choice of the reference frame. [31]

As a further consistency check, we have performed explicit calculations of BN nanotubes of increasing radius R , and extracted the voltage drop between their interior and exterior, ΔV , at the clamped-ion level. In Figure 2 we plot the estimated flexovoltage, given by $R \Delta V$, as a function of R . The asymptotic convergence to the linear-response value of φ^{CI} is clear, consistent with Eq. (1). The convergence rate, however, appears rather slow: at the largest value of R , corresponding to a nanotube primitive cell of 128 atoms, the deviation from φ^{CI} is still of about 10%. This result highlights the difficulties at calculating flexovoltages in 2D systems by using the direct approach; conversely, our method provides an optimally

converged solution within few minutes on a modern workstation, and is ideally suited, e.g. for high-throughput screening applications.

The implications of our findings for the interpretation of the experiments are best discussed in terms of the interaction between the flexural modes of a flat layer and an external, generally inhomogeneous, out-of-plane electric field, $\mathcal{E}_z(x, y)$. In full generality, Eq. (2) leads to the following coupling (energy per unit area),

$$E_{\text{flexo}}(u_z, \mathcal{E}_z) = \mu^{2D} \mathcal{E}_z \nabla^2 u_z, \quad (13)$$

which reduces to $E_{\text{flexo}} = -q^2 \mu^{2D} \mathcal{E}_z u_z$ for monochromatic fields of the type $A(x, y) = A \cos(\mathbf{q} \cdot \mathbf{r})$ [$A = (u_z, \mathcal{E}_z)$]. By deriving E_{flexo} with respect to the displacement u_z we obtain the *converse* flexoelectric effect, in the form of a vertical force per unit area, $\mathcal{F}_z = q^2 \mu^{2D} \mathcal{E}_z$, in response to the field. Explicit first-principles calculations of a BN layer under an applied \mathcal{E}_z [31] nicely confirm this prediction: Eq. (13) is the main source of out-of-plane electromechanical response in this class of materials. Note that the *longitudinal* out-of-plane flexoelectric coefficient of a free-standing layer, which we extract as a by-product of our main calculations, always vanishes (see Ref. 31) due to translational invariance and thus cannot contribute to the coupling, contrary to the common belief. [7, 8].

This allows us to generalize the existing models [37] of supported 2D layers by incorporating flexoelectricity, and thereby extract two important messages. [31] First, the amplitude of the response is highly sensitive to the substrate interaction strength, g , consistent with the results of recent measurements performed on suspended layers. [11] Second, the response displays a strong dispersion in q , indicating a marked sensitivity on the length scale of the inhomogeneities in the applied field. Both outcomes call for a reinterpretation of the existing PFM measurements of flexoelectricity: [7] information about g and the tip geometry appears essential for a quantitative estimation of μ^{2D} . We hope that our results will stimulate further experimental research along these lines, and more generally to facilitate the design of piezoelectric nanocomposites [38] based on the flexoelectric effect.

We acknowledge the support of Ministerio de Economía, Industria y Competitividad (MINECO-Spain) through Grants No. MAT2016-77100-C2-2-P and No. SEV-2015-0496, and of Generalitat de Catalunya (Grant No. 2017 SGR1506). This project has received funding from the European Research Council (ERC) under the European Union's Horizon 2020 research and innovation program (Grant Agreement No. 724529). Part of the calculations were performed at the Supercomputing Center of Galicia (CESGA).

-
- [1] Wenzhuo Wu, Lei Wang, Yilei Li, Fan Zhang, Long Lin, Simiao Niu, Daniel Chenet, Xian Zhang, Yufeng Hao, Tony F. Heinz, James Hone, and Zhong Lin Wang, "Piezoelectricity of single-atomic-layer MoS₂ for energy conversion and piezotronics," *Nature* **514**, 470–474 (2014).
 - [2] Fatemeh Ahmadpoor and Pradeep Sharma, "Flexoelectricity in two-dimensional crystalline and biological membranes," *Nanoscale* **7**, 16555–16570 (2015).
 - [3] Sergei V. Kalinin and Vincent Meunier, "Electronic flexoelectricity in low-dimensional systems," *Phys. Rev. B* **77**, 033403 (2008).
 - [4] Leo J. McGilly, Alexander Kerelsky, Nathan R. Finney, Konstantin Shapovalov, En-Min Shih, Augusto Ghiotto, Yihang Zeng, Samuel L. Moore, Wenjing Wu, Yusong Bai, Kenji Watanabe, Takashi Taniguchi, Massimiliano Stengel, Lin Zhou, James Hone, Xiaoyang Zhu, Dmitri N. Basov, Cory Dean, Cyrus E. Dreyer, and Abhay N. Pasupathy, "Visualization of Moiré superlattices," *Nature Nanotechnology* **15**, 580–584 (2020).
 - [5] Ivan Naumov, Alexander M. Bratkovsky, and V. Ranjan, "Unusual flexoelectric effect in two-dimensional non-centrosymmetric *sp*²-bonded crystals," *Phys. Rev. Lett.* **102**, 217601 (2009).
 - [6] Karel-Alexander N. Duerloo, Mitchell T. Ong, and Evan J. Reed, "Intrinsic piezoelectricity in two-dimensional materials," *The Journal of Physical Chemistry Letters* **3**, 2871–2876 (2012).
 - [7] Christopher J. Brennan, Rudresh Ghosh, Kalhan Koul, Sanjay K. Banerjee, Nanshu Lu, and Edward T. Yu, "Out-of-plane electromechanical response of monolayer molybdenum disulfide measured by piezoresponse force microscopy," *Nano Letters* **17**, 5464–5471 (2017).
 - [8] Christopher J. Brennan, Kalhan Koul, Nanshu Lu, and Edward T. Yu, "Out-of-plane electromechanical coupling in transition metal dichalcogenides," *Applied Physics Letters* **116**, 053101 (2020).
 - [9] P. Zubko, G. Catalan, and A. K. Tagantsev, "Flexoelectric effect in solids," *Annu. Rev. Mater. Res.* **43**, 387–421 (2013).
 - [10] Bo Wang, Yijia Gu, Shujun Zhang, and Long-Qing Chen, "Flexoelectricity in solids: Progress, challenges, and perspectives," *Progress in Materials Science* **106**, 100570 (2019).
 - [11] Xiang Wang, Anyang Cui, Fangfang Chen, Liping Xu, Zhigao Hu, Kai Jiang, Liyan Shang, and Junhao Chu, "Probing effective out-of-plane piezoelectricity in van der waals layered materials induced by flexoelectricity," *Small* **15**, 1903106 (2019).
 - [12] T. Jungk, Á. Hoffmann, and E. Soergel, "Influence of the inhomogeneous field at the tip on quantitative piezoresponse force microscopy," *Applied Physics A* **86**, 353–355 (2007).
 - [13] Wenhao Shi, Yufeng Guo, Zhuhua Zhang, and Wanlin Guo, "Flexoelectricity in monolayer transition metal dichalcogenides," *The Journal of Physical Chemistry Letters* **9**, 6841–6846 (2018).
 - [14] Wenhao Shi, Yufeng Guo, Zhuhua Zhang, and Wanlin Guo, "Strain gradient mediated magnetism and polarization in monolayer VSe₂," *J. Phys. Chem. C* **123**, 24988–24993 (2019).

- [15] T. Pandey, L. Covaci, and F.M. Peeters, “Tuning flexoelectricity and electronic properties of zig-zag graphene nanoribbons by functionalization,” *Carbon* **171**, 551–559 (2021).
- [16] T. Pandey, L. Covaci, M. V. Milošević, and F. M. Peeters, “Flexoelectricity and transport properties of phosphorene nanoribbons under mechanical bending,” *Phys. Rev. B* **103**, 235406 (2021).
- [17] Xiaoying Zhuang, Bo He, Brahmanandam Javvaji, and Harold S. Park, “Intrinsic bending flexoelectric constants in two-dimensional materials,” *Phys. Rev. B* **99**, 054105 (2019).
- [18] Brahmanandam Javvaji, Bo He, Xiaoying Zhuang, and Harold S. Park, “High flexoelectric constants in janus transition-metal dichalcogenides,” *Phys. Rev. Materials* **3**, 125402 (2019).
- [19] David Codony, Irene Arias, and Phanish Suryanarayana, “Transversal flexoelectric coefficient for nanostructures at finite deformations from first principles,” *Phys. Rev. Materials* **5** (2021), 10.1103/physrevmaterials.5.1030801.
- [20] M. Stengel, “Microscopic response to inhomogeneous deformations in curvilinear coordinates,” *Nature Communications* **4**, 2693 (2013).
- [21] L. Eric Cross, “Flexoelectric effects: Charge separation in insulating solids subjected to elastic strain gradients,” *Journal of Materials Science* **41**, 53–63 (2006).
- [22] P. V. Yudin and A. K. Tagantsev, “Fundamentals of flexoelectricity in solids,” *Nanotechnology* **24**, 432001 (2013).
- [23] Raffaele Resta, “Towards a bulk theory of flexoelectricity,” *Phys. Rev. Lett.* **105**, 127601 (2010).
- [24] M. Stengel, “Flexoelectricity from density-functional perturbation theory,” *Phys. Rev. B* **88**, 174106 (2013).
- [25] Massimiliano Stengel and David Vanderbilt, “First-principles theory of flexoelectricity,” in *Flexoelectricity in Solids From Theory to Applications*, edited by Alexander K. Tagantsev and Petr V. Yudin (World Scientific Publishing Co., Singapore, 2016) Chap. 2, pp. 31–110.
- [26] Cyrus E. Dreyer, Massimiliano Stengel, and David Vanderbilt, “Current-density implementation for calculating flexoelectric coefficients,” *Phys. Rev. B* **98**, 075153 (2018).
- [27] Andrea Schiaffino, Cyrus E. Dreyer, David Vanderbilt, and Massimiliano Stengel, “Metric wave approach to flexoelectricity within density functional perturbation theory,” *Phys. Rev. B* **99**, 085107 (2019).
- [28] Miquel Royo and Massimiliano Stengel, “First-principles theory of spatial dispersion: Dynamical quadrupoles and flexoelectricity,” *Phys. Rev. X* **9**, 021050 (2019).
- [29] Aldo H. Romero, Douglas C. Allan, Bernard Amadon, Gabriel Antonius, Thomas Applencourt, Lucas Baguet, Jordan Bieder, François Bottin, Johann Bouchet, Eric Bousquet, Fabien Bruneval, Guillaume Brunin, Damien Caliste, Michel Côté, Jules Denier, Cyrus Dreyer, Philippe Ghosez, Matteo Giantomassi, Yannick Gillet, Olivier Gingras, Donald R. Hamann, Geoffroy Hautier, François Jollet, Gérard Jomard, Alexandre Martin, Henrique P. C. Miranda, Francesco Naccarato, Guido Petretto, Nicholas A. Pike, Valentin Planes, Sergei Prokhorenko, Tonatiuh Rangel, Fabio Ricci, Gian-Marco Rignanese, Miquel Royo, Massimiliano Stengel, Marc Torrent, Michiel J. van Setten, Benoit Van Troeye, Matthieu J. Verstraete, Julia Wiktor, Josef W. Zwanziger, and Xavier Gonze, “Abinit: Overview and focus on selected capabilities,” *The Journal of Chemical Physics* **152**, 124102 (2020).
- [30] Richard M. Martin, “Piezoelectricity,” *Phys. Rev. B* **5**, 1607–1613 (1972).
- [31] See Supplemental Material at <http://link> for more information about theoretical derivations, computational details and results, which includes Refs. [39–48].
- [32] Massimiliano Stengel, “Surface control of flexoelectricity,” *Phys. Rev. B* **90**, 201112 (2014).
- [33] Jiawang Hong and David Vanderbilt, “First-principles theory and calculation of flexoelectricity,” *Phys. Rev. B* **88**, 174107 (2013).
- [34] S. Baroni, S. de Gironcoli, and A. Dal Corso, “Phonons and related crystal properties from density-functional perturbation theory,” *Rev. Mod. Phys.* **73**, 515 (2001).
- [35] X. Gonze and C. Lee, “Dynamical matrices, Born effective charges, dielectric permittivity tensors, and interatomic force constants from density-functional perturbation theory,” *Phys. Rev. B* **55**, 10355 (1997).
- [36] X. Gonze, B. Amadon, P.-M. Anglade, J.-M. Beuken, F. Bottin, P. Boulanger, F. Bruneval, D. Caliste, R. Caracas, M. Côté, T. Deutsch, L. Genovese, Ph. Ghosez, M. Giantomassi, S. Goedecker, D.R. Hamann, P. Hermet, F. Jollet, G. Jomard, S. Leroux, M. Mancini, S. Mazevet, M.J.T. Oliveira, G. Onida, Y. Pouillon, T. Rangel, G.-M. Rignanese, D. Sangalli, R. Shaltaf, M. Torrent, M.J. Verstraete, G. Zerah, and J.W. Zwanziger, “ABINIT: First-principles approach to material and nanosystem properties,” *Computer Phys. Commun.* **180**, 2582–2615 (2009).
- [37] Bruno Amorim and Francisco Guinea, “Flexural mode of graphene on a substrate,” *Phys. Rev. B* **88**, 115418 (2013).
- [38] Baojin Chu, Wenyi Zhu, Nan Li, and L. Eric Cross, “Flexure mode flexoelectric piezoelectric composites,” *Journal of Applied Physics* **106**, 104109 (2009).
- [39] Miquel Royo, Konstanze R Hahn, and Massimiliano Stengel, “Using high multipolar orders to reconstruct the sound velocity in piezoelectrics from lattice dynamics,” *Phys. Rev. Lett.* **125**, 217602 (2020).
- [40] D. R. Hamann, “Optimized norm-conserving vanderbilt pseudopotentials,” *Phys. Rev. B* **88**, 085117 (2013).
- [41] M.J. van Setten, M. Giantomassi, E. Bousquet, M.J. Verstraete, D.R. Hamann, X. Gonze, and G.-M. Rignanese, “The PseudoDojo: Training and grading a 85 element optimized norm-conserving pseudopotential table,” *Comp. Phys. Comm.* **226**, 39–54 (2018).
- [42] K.S. Novoselov, A. Mishchenko, A. Carvalho, and A.H. Castro Neto, “2d materials and van der waals heterostructures,” *Science* **353**, aac9439 (2016).
- [43] Nicholas A. Pike, Benoit Van Troeye, Antoine Dewandre, Guido Petretto, Xavier Gonze, Gian-Marco Rignanese, and Matthieu J. Verstraete, “Origin of the counterintuitive dynamic charge in the transition metal dichalcogenides,” *Phys. Rev. B* **95**, 201106 (2017).
- [44] John P. Perdew, Kieron Burke, and Matthias Ernzerhof, “Generalized gradient approximation made simple,” *Phys. Rev. Lett.* **77**, 3865–3868 (1996).
- [45] D.R. Hamann, Karin M. Rabe, and David Vanderbilt, “Generalized-gradient-functional treatment of strain in density-functional perturbation theory,” *Phys. Rev. B* **72** (2005), 10.1103/physrevb.72.033102.
- [46] Anubhav Jain, Shyue Ping Ong, Geoffroy Hautier, Wei Chen, William Davidson Richards, Stephen Dacek, Shreyas Cholia, Dan Gunter, David Skinner, Gerbrand

- Ceder, and Kristin A. Persson, “The materials project: A materials genome approach to accelerating materials innovation,” *APL Materials* **1**, 011002 (2013).
- [47] Miquel Royo and Massimiliano Stengel, “Exact long-range dielectric screening and interatomic force constants in quasi-2d crystals,” *Physical Review X* (accepted), arXiv preprint arXiv:2012.07961 (2020).
- [48] Shashikant Kumar and Phanish Suryanarayana, “Bending moduli for forty-four select atomic monolayers from first principles,” *Nanotechnology* **31**, 43LT01 (2020).